Fermi National Accelerator Laboratory

FERMILAB-Conf-93/352-E
DØ

B Production and $B^0\bar{B}^0$ Mixing at DØ

Dmitri Denisov
For the DØ Collaboration

Fermi National Accelerator Laboratory
P.O. Box 500, Batavia, Illinois 60510

SSC Laboratory
2550 Beckleymeade Ave., Dallas, Texas 75237

November 1993

Published Proceedings *Advanced Study Conference on: Heavy Flavours*, Pavia, Italy, September 3-7, 1993

Operated by Universities Research Association Inc. under Contract No. DE-AC02-76CHO3000 with the United States Department of Energy

Disclaimer

B PRODUCTION AND $B^0\bar{B}^0$ MIXING AT D0

Dmitri Denisov
for the D0 collaboration
Superconducting Supercollider Laboratory
2550 Beckleymeade ave., Dallas, Texas, 75237

Abstract

Preliminary results on B physics studies from the D0 experiment at the Fermilab collider are presented. Single and dimuon events produced in $p\bar{p}$ collisions at $\sqrt{s} = 1.8$ TeV were used in the analysis. Inclusive single muon and J/ψ differential cross sections are shown. The results of a measurement of the time averaged $B^0\bar{B}^0$ mixing parameter are presented.

Published Proceedings *Advanced Study Conference on: Heavy Flavours*, Pavia (Italy), September, 3-7, 1993.

Introduction

The D0 detector collected its first data sample in the 1992-1993 collider run at Fermilab. Most of the run was devoted to physics emphasizing top quark searches and electroweak physics. Not specially optimized for B physics studies, D0 can investigate some physics associated with B production dynamics and $B^0\bar{B}^0$ mixing using large $(10^{-3}\sigma_{tot})$ $b\bar{b}$ cross section at $\sqrt{s}$ = 1.8 TeV and the unique features of the D0 muon system.

D0 detector

The D0 detector consists of central tracking and transition radiation detectors, a uranium-liquid argon calorimeter and a muon detection system. Details of the D0 detector design and its performance are given in reference [1]). The results presented here were obtained using muons detected by the D0 detector. The muon system consists of iron toroids with an average magnetic field of 1.8 T and 3 layers of 10 cm wide proportional drift tubes as coordinate detectors. A Small Angle MUon System (SAMUS) consisting of 3 cm diameter proportional drift tubes extends the η coverage of the muon system to $|\eta| = 3.3$. The absence of a central magnetic field in the D0 detector limits the muon momentum resolution (due to multiple scattering) to 18%. The momentum resolution of the SAMUS spectrometer is presented in Fig. 1. The thickness of the calorimeter plus iron toroids is 14-18 interaction lengths which provides small punchthrough probability (10^{-4}) and permits good muon identification within a jet.

The central tracking chambers play an important role in muon identification by matching tracks found by the muon system with tracks reconstructed near the interaction vertex. The D0 calorimeter covers η up to 4 and has a good energy resolution and fine segmentation for good measurement of jet energies. The low noise of the calorimeter provides effective detection of minimum ionizing particles thus diminishing the background in muon detection.

Inclusive single muon cross sections

The D0 multi-level trigger system reduces 43 mb of inelastic cross section to 2 Hz of interesting events which are written to tape. The following set of triggers was used during data collection for single muon studies. Level 0 trigger (scintillator counters) selected the beam crossing with an inelastic collision. The Level 1 hardware trigger selected events with a hit pattern in the muon detector consistent with at least one muon candidate with $p_t^{\mu} > 3$ GeV/c. The Level 2 software trigger which used all digitized information about the event and made preliminary track reconstruction selected events with at least one track with $p_t^{\mu} > 3$ GeV/c $(|\eta| < 1.6)$ or $p_t^{\mu} > 1$ GeV/c $(2.2 < |\eta| < 3.3)$. Due to the high rate of single muon triggers

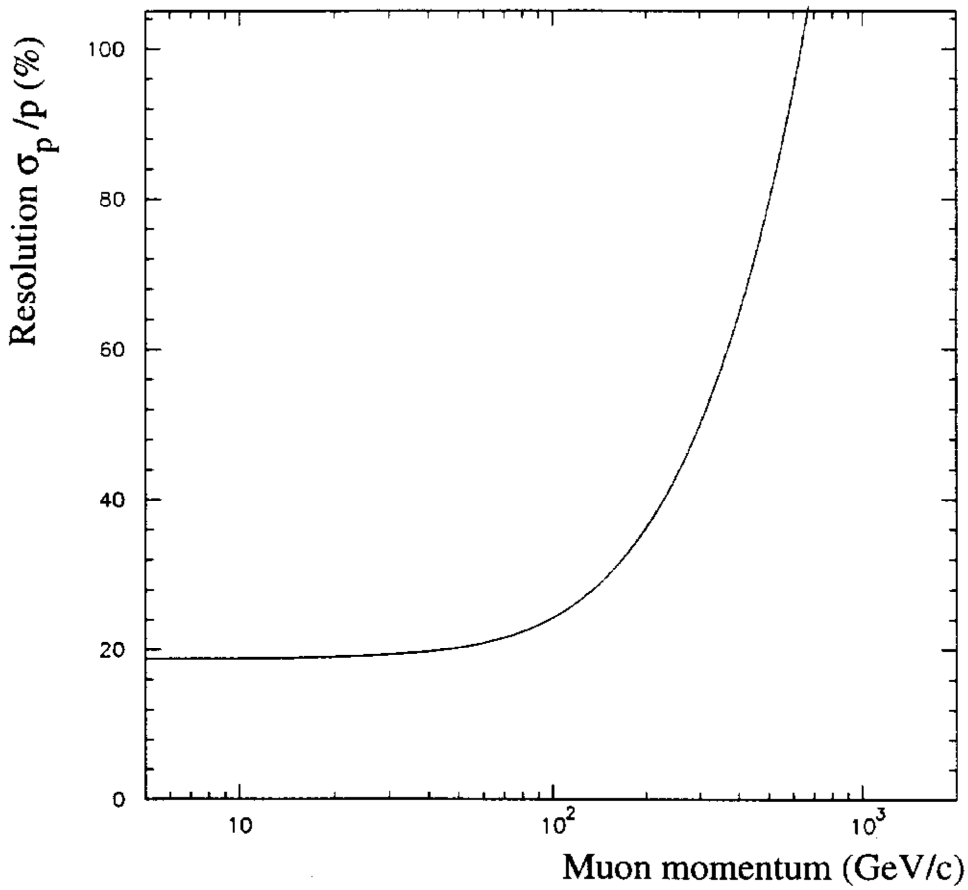

Fig. 1. Momentum resolution of the SAMUS spectrometer

data for the inclusive single muon cross section measurement were taken in several "special" runs. Data were collected for 3 different regions $|\eta| < 1.0$, $1.0 < |\eta| < 1.6$, and $2.2 < |\eta| < 3.3$ with integrated luminosities of 89 nb^{-1}, 11 nb^{-1} and 5 nb^{-1} respectively.

After track reconstruction the following off-line cuts to reject backgrounds were applied:

1. Hits on track in all 3 layers of the muon chambers.
2. > 1 GeV energy deposition along track in the calorimeter.
3. Match with central detector track ($|\eta| < 1.6$ only).
4. Cosmic ray rejection cuts.

The overall efficiency of single muon detection was calculated using single muon Monte Carlo events. These events were passed through the full GEANT detector simulation, Level 1 and Level 2 trigger simulators, reconstruction and off-line cuts. In Fig. 2 the detection efficiency (including geometrical acceptance) is presented for the three different η regions.

The inclusive single muon cross section is calculated by dividing the number of observed muons in a given p_t bin by the efficiency, integrated luminosity and η interval. Positive and negative muons were counted together. The results for different η regions are presented in Figs. 3(a,b,c). Different contributions to the cross section obtained using an ISAJET simulation are also shown in Figs. 3. The absolute normalization of the cross section is limited by the accuracy of the luminosity measurement, the accuracy of efficiency estimation and background (cosmic, combinatoric) subtraction. The estimated systematic error of the cross section measurement is 25%. The smaller error bars in Figs. 3 represent statistical errors only, the larger - systematic and statistical combined. The data agree within errors with the summed contributions from ISAJET. The extraction of the $b\bar{b}$ cross section from the inclusive single muon data is in progress.

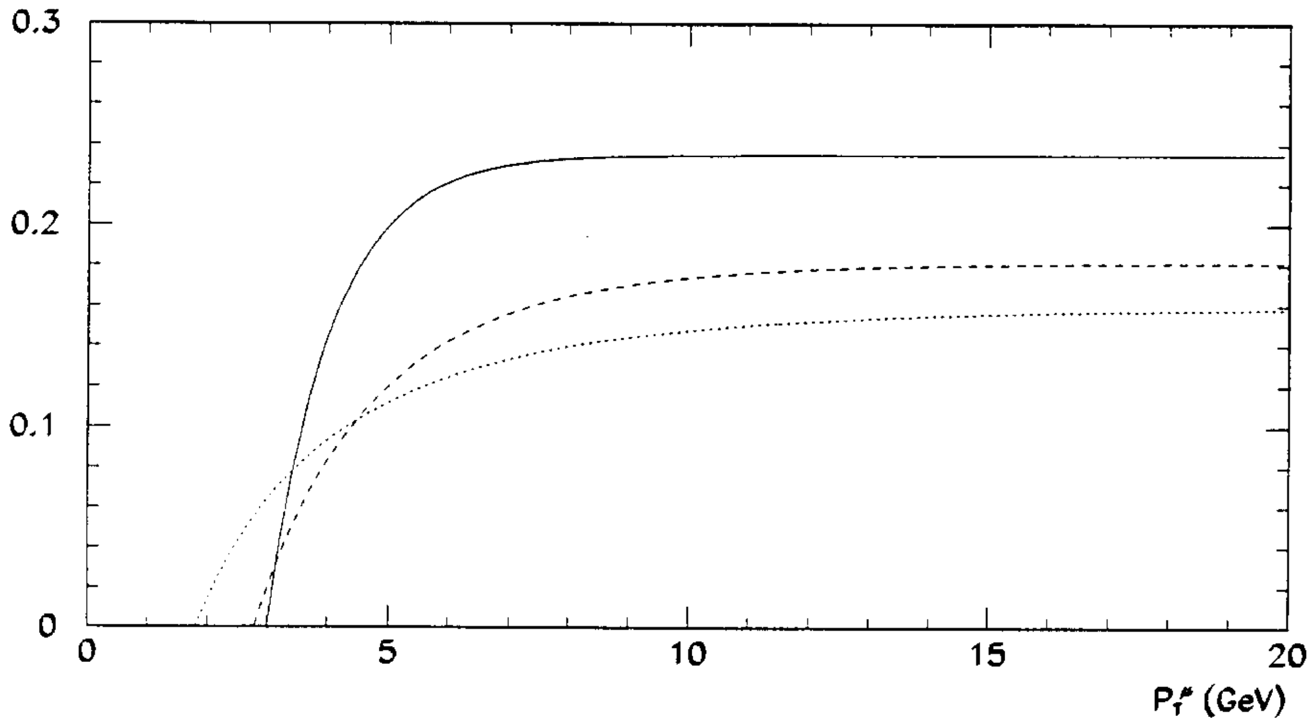

Fig. 2. Efficiency of muon detection for different η regions: $|\eta| < 1.0$ - solid curve, $1.0 < |\eta| < 1.6$ - dashed curve, $2.2 < |\eta| < 3.3$ - dotted curve

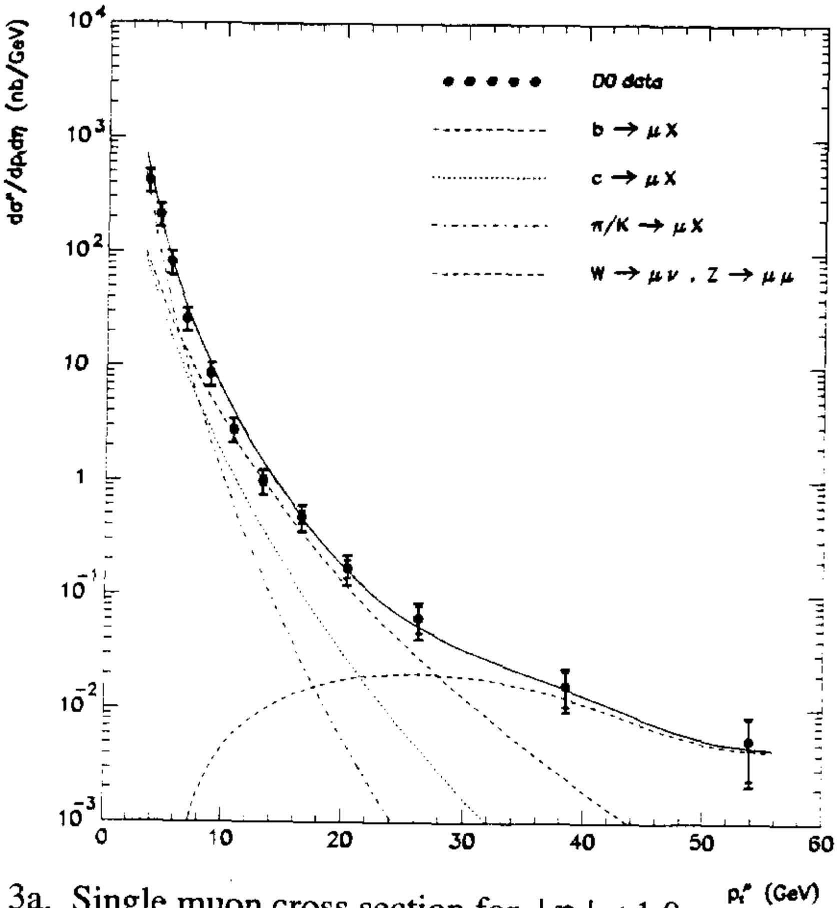

Fig. 3a. Single muon cross section for $|\eta| < 1.0$

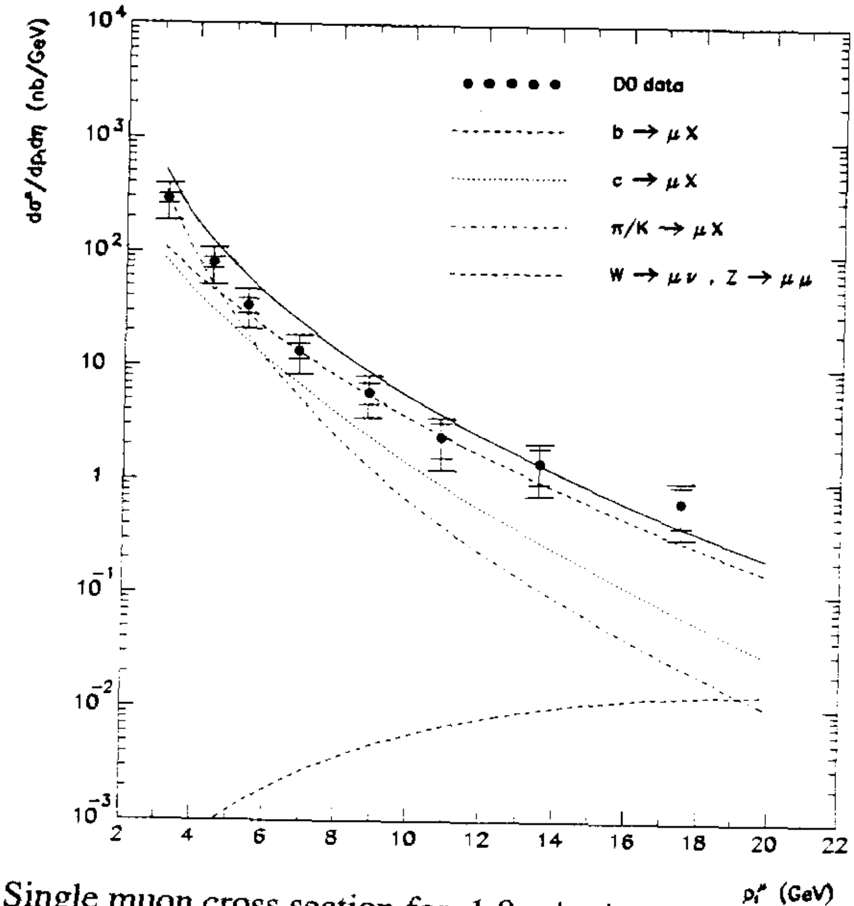

Fig. 3b. Single muon cross section for $1.0 < |\eta| < 1.6$

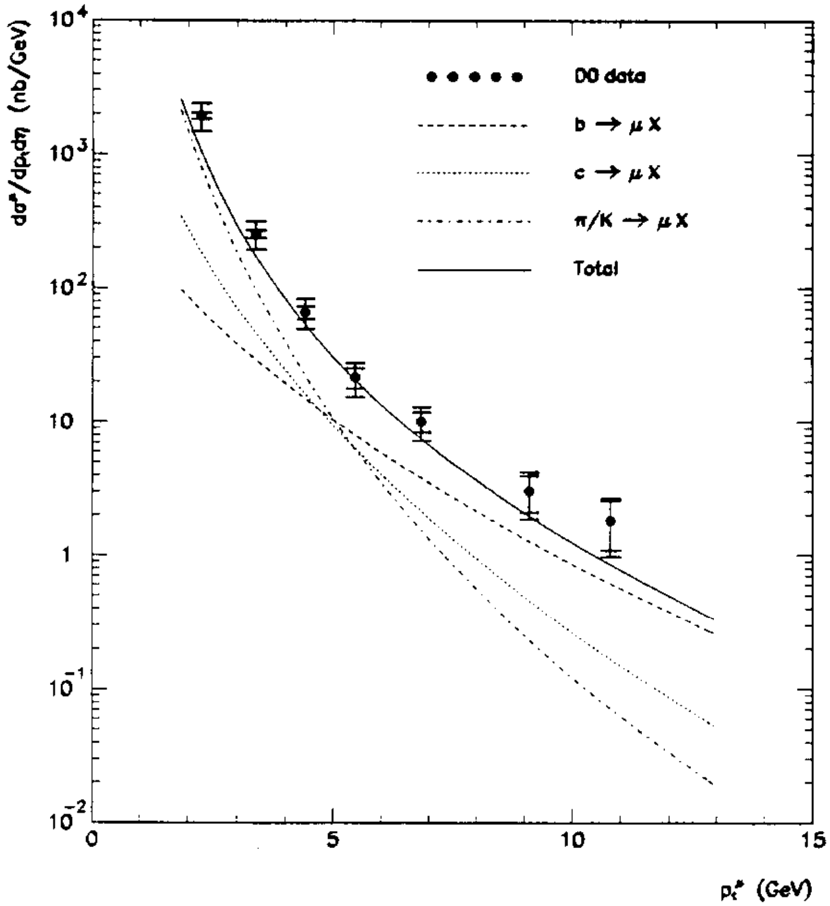

Fig. 3c. Single muon cross section for $2.2 < |\eta| < 3.3$

Inclusive J/ψ cross section measurement

The data for the dimuon analysis were collected with requirements of inelastic interaction (Level 0 trigger), ⩾2 muons found by Level 1 trigger and ⩾2 muons reconstructed by Level 2 trigger. The integrated luminosity of the data sample used in this J/ψ cross section measurement is 3.5 pb^{-1}.

After track reconstruction the following off-line cuts to reject backgrounds were applied:

1. At least 2 muon tracks.
2. > 1 GeV energy deposition along track in the calorimeter.
3. Dimuon $p_t > 8$ GeV/c.
4. Cosmic ray rejection cuts.
5. $|\eta| < 0.8$ for both muons.

The dimuon invariant mass spectra for like and unlike sign dimuons and for isolated and non-isolated samples are shown in Figs. 4 (a,b).

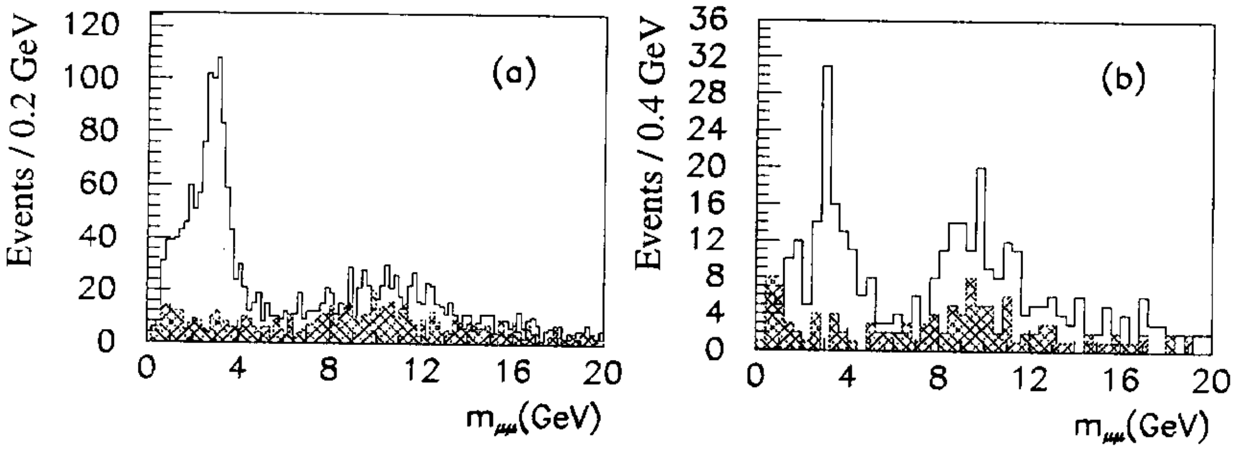

Fig. 4. Unlike sign (unshaded) and like sign (shaded) invariant mass for: (a) non-isolated and (b) isolated dimuons

Isolated dimuons are defined to be muon pairs with $\Delta R = \sqrt{\Delta\eta^2 + \Delta\phi^2}$ between each muon and nearest jet greater than 0.7. The jet is defined using a $\Delta R = 0.7$ and has $E_t > 8$ GeV. Non-isolated dimuons have at least one muon within $\Delta R = 0.7$ about nearest jet. Neither like sign sample shows evidence of mass peaks. Both unlike sign samples show a clear J/ψ peak. The Υ peak exists in the isolated unlike sign spectrum which indicates its direct production. Both isolated and non-isolated dimuons were used for the inclusive J/ψ cross section determination. The number of J/ψ's in each p_t bin was estimated by fitting the mass distribution to a Gaussian (signal) plus a polynomial (background). The efficiency of J/ψ detection was estimated by generating events with J/ψ 's using ISAJET Monte Carlo, passing them through GEANT and trigger simulators, reconstructing and passing them through off-line cuts. The efficiency for J/ψ detection is around 10% for $p_t^{J/\psi} > 15$ GeV/c.

The inclusive cross section for J/ψ production is shown in Fig. 5. To calculate the cross section the number of J/ψ in each p_t bin was divided by the efficiency, integrated luminosity and η range. The errors shown in Fig. 5 are only statistical. The systematic uncertainty is around 50%. In Fig. 5 the predictions [2-4]) for J/ψ's from direct production (CPM) and for J/ψ's from B decay (BPM) are shown. For the low p_t region the data lie above the summed contributions, although the 50%

systematic errors mean that this observation is not meaningful statistically. The extraction of bb cross section from inclusive J/ψ's data is in progress with the aim of reducing the systematic error to the 10% level.

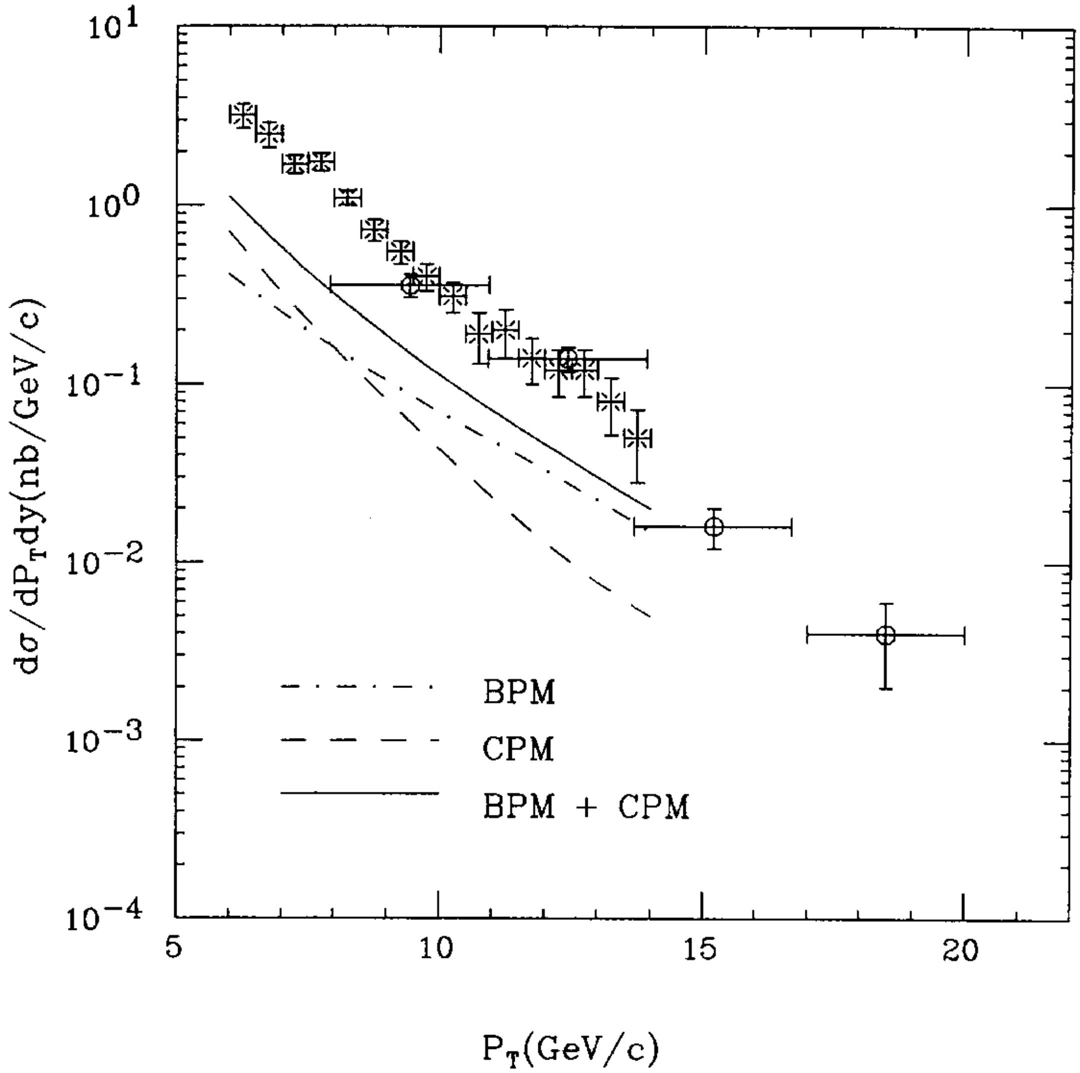

Fig. 5. Inclusive J/ψ cross section: 0 - D0 results, * - CDF results [5])

$B^0\bar{B}^0$ mixing studies

The semi-leptonic decay of both mesons from $B^0\bar{B}^0$ pair into muons will produce unlike sign dimuons. Flavor mixing of a B^0 or $\bar{B}^0$ will result in like sign dimuons. Like sign dimuons can also be produced in uncorrelated decays of light quarks. In the presence of mixing the fraction of like and unlike sign dimuons for various processes is given in Table 1 where χ is the mixing parameter averaged over time and combined for B_s and B_d mesons.

Table 1

The fraction of like and unlike sign dimuons for various processes

	Process	Like sign	Unlike sign
P1	$b \to \mu^-$, $\bar{b} \to \mu^+$	$2\chi(1-\chi)$	$(1-\chi)^2+\chi^2$
P2	$b \to \mu^-$, $\bar{b} \to \bar{c} \to \mu^-$	$(1-\chi)^2+\chi^2$	$2\chi(1-\chi)$
P3	$b \to c \to \mu^+$, $\bar{b} \to \bar{c} \to \mu^-$	$2\chi(1-\chi)$	$(1-\chi)^2+\chi^2$
P4	$b \to c\mu^-$, $c \to \mu^+$	0%	100%
P5	$c \to \mu^+$, $\bar{c} \to \mu^-$	0%	100%
P6	Drell-Yan, J/ψ, Υ	0%	100%
P7	Decay background	50%	50%

The data for the mixing parameter studies were collected with the dimuon triggers described above. Integrated luminosity corresponding to analyzed data sample is 8.4 pb^{-1}. The following off-line cuts were used to enrich the sample with events from $B^0\bar{B}^0$ decays and to enhance "leading" dimuons.

1. 2 or 3 muon tracks in $|\eta| < 1.1$.

2. > 1 GeV energy deposition along track in the calorimeter.

3. Cosmic ray rejection cuts.

4. Muon pair invariant mass > 6 GeV/c^2 - to remove J/ψ's.

5. 2 GeV/c < p_t^{μ} < 25 GeV/c - ensures proper muon sign determination.

Each event has at least one jet with $E_t^{jet} > 8$ GeV within $\Delta R = 0.8$ of the muon. All muons which have an associated jet must have $p_t^{rel} > 1.2$ GeV/c relative to the jet axis. These cuts are used to enhance events with leading dimuons coming from B mesons decays. After these cuts 116 like sign and 234 unlike sign events were found. Around 15% of events in this sample are cosmic ray background. The final ratio of like to unlike sign dimuon pairs is equal to:

$$R = 0.51 \pm 0.06(stat) \pm 0.02(syst) \quad (1)$$

where the systematic error is associated with uncertainties in the cosmic ray background. In order to extract the χ parameter from the experimentally measured ratio R it is necessary to know the contributions of all the processes from Table 1. For this we used the ISAJET Monte Carlo event generator and fast detector simulator. The trigger simulators and off-line cuts listed above were applied and the relative fractions of contributing processes are shown in Table 2. The errors in Table 2 are statistical errors due to limited Monte Carlo statistics.

Table 2

The relative fractions of the contributing processes for dimuon pair production

Process from Table 1	Fraction
P1	0.66+-0.15
P2	0.15+-0.06
P3	0.09+-0.04
P4-P6	0.02+-0.02
P7	0.08+-0.04

Using (1) and relative fractions from Table 2 we find for the combined time averaged mixing parameter :

$$\chi = 0.14 \pm 0.03(stat) \pm 0.06(syst) \quad (2)$$

The systematic error is dominated by uncertainties in the fractions of the contributing processes. The χ value is in good agreement with results from CDF and LEP [6-11]). We continue to work on reducing the systematic error by increasing the Monte Carlo statistics and improving the analysis technique.

Conclusions

The D0 experiment has produced preliminary results on the inclusive muon cross section for $|\eta| < 3.3$, inclusive J/ψ production cross section and measurement of the time averaged mixing parameter in $p\bar{p}$ collisions at $\sqrt{s} = 1.8$ TeV. We continue the analysis of collected data to include the full available data set, obtain the b-quark cross section, constrain the gluon density distributions at small x $(x = 10^{-3})$ using muon cross section at high η. The analysis of events with such particles as γ's and K^0's associated with J/ψ's is in progress. We are planning to increase our statistics for B physics studies by an order of magnitude in the next Fermilab collider run in 1994 using the larger luminosity and improved trigger system.

References

1. S. Abachi et al., FNAL Preprint Pub-93/179-E, 1993.
2. E.W.N. Glover et al., Z. Phys. C38(1988)473.
3. P. Nason et al., Nucl. Phys. B303(1988)607.
4. C. Peterson et al., Phys. Rev. D27(1983)105.
5. V. Papadimitrou et al., FNAL Preprint Conf-92/252-E, 1992.
6. C. Albajar et. al., Phys. Lett. B262(1991)171.
7. F. Abe et. al., Phys. Rev. Lett. 67(1991)3351.
8. B. Adeva et al., Phys. Lett. B288(1992)395.
9. D. Decamp et al., Phys. Lett. B236(1991)236.
10. P. Acton et al., Phys. Lett. B276(1992)379.
11. P. Abreu et al., Phys. Lett. B301(1993)345.